JOURNAL OF SOLID STATE CHEMISTRY 72, 316–323 (1988)

Photoelectronic Properties of the *p*-type Layered Trichalcogenophosphates $FePS_3$ and $FePSe_3$

A. ARUCHAMY, H. BERGER, AND F. LEVY

Institut de Physique Appliquee, Ecole Polytechnique Federale de Lausanne, CH-1015 Lausanne, Switzerland

Received February 5, 1987; in revised form June 8, 1987

The *p*-type as grown single crystals of the layered compounds $FePS_3$ and $FePSe_3$ have been studied by the photoelectrochemical method. The current–voltage and capacitance–voltage characteristics indicate the presence of surface states. The analysis of the photocurrent quantum efficiencies give two indirect optical transitions at 1.62 and 2.3 eV for $FePS_3$ and at 1.3 and 1.83 eV for $FePSe_3$. Hole mobilities are in the range 0.5–1.0 $cm^2\ V^{-1}\ sec^{-1}$ as found from the Hall effect measurements. These results are interpreted in terms of the existing electronic band scheme for the MPX_3 (M = transition metal; X = S, Se) layer compounds. © 1988 Academic Press, Inc.

Introduction

The layered chalcogenophosphates of the general formula MPX_3 (M = transition metal; X = S, Se) have been the subject of considerable interest in recent years (*1–3*) due to their possible use as cathode materials in room temperature lithium batteries comparable to TiS_2 (*4*) and for intercalation reactions in general (*5*). The similarity between these ternary compounds and the layered transition metal dichalcogenides appears from the fact that the MPX_3 compounds can be described as substitution of one third of the metal by P–P (P_2) groups in the MX_2 formula, i.e., $M_{2/3}(P_2)_{1/3}X_2$ (*3, 6*). Electrical and optical studies have indicated that they are semiconductors with wide band gaps ranging from 1.3 eV to more than 3 eV (*3, 7*). Magnetic studies have shown that they are antiferromagnetic and that the *d*-electrons of the transition metal ions are strongly localized (*3*). Electronic conduction mechanism in doped samples of $NiPS_3$ has been recently examined (*8*). Empirical energy band schemes have been derived for MPX_3 compounds based on several optical and electron spectroscopic studies (*9–11*).

In this paper we report on photoelectrochemical (PEC) measurements on the *p*-type as grown semiconducting $FePS_3$ and $FePSe_3$ whose fundamental absorption edges have been reported at 1.5 and 1.3 eV, respectively (*3*). The appreciable conductivity ($>10^{-5}$ $ohm^{-1}\ cm^{-1}$) in the undoped materials grown by sublimation has been attributed to nonstoichiometry (~0.1% iron deficiency) (*8*). The characteristics of semiconductor electrodes in photoelectrochemical cells depend on the structure, on the bulk electronic parameters of the material, and on the surface properties (*12–16*). The investigation of the cell characteristics often provides a way of obtaining the main electronic parameters of the semiconductor

0022-4596/88 $3.00

such as the fundamental optical transition and its nature, the diffusion length of the minority carrier, etc. (*16–20*). The reported values of their optical absorption edges indicate that these compounds can be used, in principle, as solar cell materials. Therefore, an evaluation of the energy conversion parameters in a PEC cell is appropriate. Earlier studies (*21–23*) on some of the MPX_3 compounds have shown significant PEC response in aqueous electrolytes. However, no detailed measurements have been reported so far on this class of materials.

Experimental

The crystals of $FePS_3$ and $FePSe_3$ were grown by chemical vapor transport reaction or by sublimation in a two-zone furnace. For both compounds the temperatures of the two zones were 720–700°C in the case of the iodine transport and 770–720°C for sublimation. The growth experiments were carried out for several days and the resulting single crystals were platelets of ~0.01–0.1 mm in thickness and ~0.5–1 cm^2 in size with black appearance. An elementary check of the thermoelectrical voltage showed that they were p-type semiconductors. Room temperature resistivities were 30 ohm-cm for $FePSe_3$ and 1000 ohm cm for $FePS_3$ as measured by the van der Pauw four-probe technique. The electrical leads were contacted with the help of a Hg–In–Ga alloy. The Hall voltage was measured in the basal plane of the crystal.

Electrochemical studies were carried out on selected crystals mounted as electrodes with Hg–In–Ga alloy for the back contact covered with a silver paste overlayer. A copper wire used as electrical lead was enclosed in a glass tube holder. The insulating mounting of the copper wire and of the back surface of the crystal was made with epoxy, leaving only the front surface of the crystal exposed to electrolyte. The electrodes were rinsed in HNO_3 for 30 sec before the experiment. A Pt foil was used as the counter electrode. An AMEL potentiostat (Model 552) with a Wenking scan generator (VSG-72) served for the current–voltage (i–v) measurements. The light source was a 150-W tungsten lamp or a 200-W high-pressure Hg lamp with a water filter. Spectral response measurements were made using a tungsten–halogen lamp source and Kratos high intensity monochromator with appropriate cutoff filters. Light intensity was measured with a thermopile radiometer. Capacitance measurements were made using a Solartron spectrum analyzer.

Results

Figure 1 shows the i–v characteristics for $FePS_3$ and $FePSe_3$ in dark and under illumination in 0.5 M H_2SO_4. Due to high resistivity of the sulfide, the photocurrents are very low and increase with applied potential without reaching saturation. The photocurrent onset for the $FePS_3$ electrode is at 0.0 V vs SCE. For $FePSe_3$, very small photocathodic currents start to flow close to −0.2 V vs SCE but a sharp rise is seen at −0.6 V vs SCE only. The dark currents are generally small but vary from sample to sample. Evolution of hydrogen is observed at the surface and no visible changes are apparent during the i–v measurements. An open circuit photovoltage of 60 mV was measured for $FePSe_3$ in H_2SO_4 (0.5 M). While H_2SO_4 may not present a well-defined redox system at the electrode/electrolyte interface, the sign and the value of the photopotential indicate a band bending at the hydrogen evolution potential. On the other hand, the current–voltage curves show only small photocurrents at potentials near the photo-onset (Fig. 1b). A steep increase of the photocurrent and hydrogen evolution take place at ~ −0.6 V vs SCE. These observations suggest a high level of

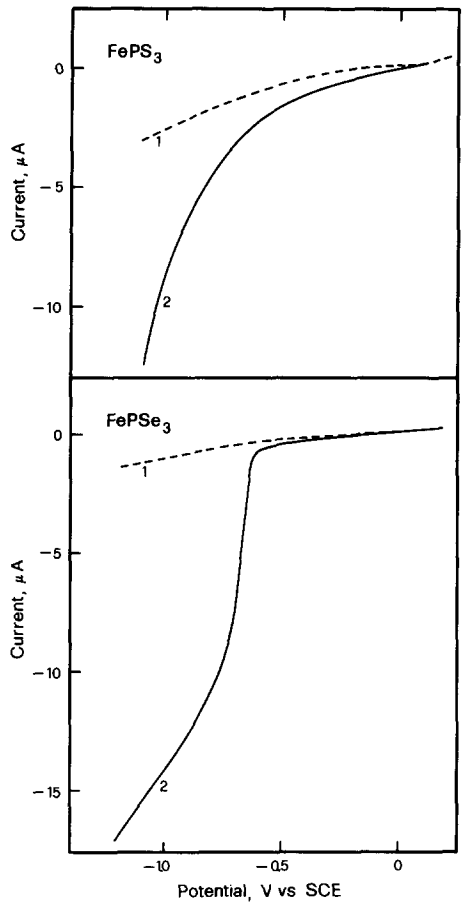

FIG. 1. Current–voltage curves in 0.5 *M* H_2SO_4 for (a) *p*-$FePS_3$ (light source, 200-W high-presure Hg lamp) and (b) *p*-$FePSe_3$ (light source, 150-W W lamp). Curve 1, dark; curve 2, light.

surface recombination. $FePSe_3$, when examined in $CuSO_4$ (0.2 *M*) electrolyte, shows (Fig. 2) a positive shift of the photoonset potential. Cu^{2+} is reduced photocathodically at the electrode surface. The deposition of Cu on the surface appears to modify the surface as seen from the subsequent i–v curves. The redox and the flatband potential considerations, however, indicate that no net energy storage is possible in these electrolytes.

$FePSe_3$ tends to decompose when an i–v run is carried out at higher pH electrolytes under illumination. A pale yellow layer is visible on the crystal after an i–v run in 1 *M* NaOH or in pH 9 electrolyte. A similar observation has been reported earlier for $FePS_3$ (*21*). The stability of the two types of electrodes was checked in 0.5 *M* H_2SO_4 under illumination, keeping the electrodes potentiostated at −0.9 V vs SCE. While the photocurrent remains constant for more than 2 hr for $FePS_3$, a small decline was noticed for $FePSe_3$ after an hour. However, no surface changes were apparent for both electrodes. It should be noted, however, that the photocurrent densities are much less at $FePS_3$. The decline in photocurrent at $FePSe_3$ can be caused by defects at the layer edges, hydrogen incorporation in the crystal at interlayer sites by photointercalation, etc.

Capacitance–voltage measurements were carried out with several electrodes of $FePSe_3$ in 0.5 *M* H_2SO_4 at different frequencies. Some frequency dispersion was observed. The Mott–Schottky plots are given in Fig. 3 and the obtained value for the flat-

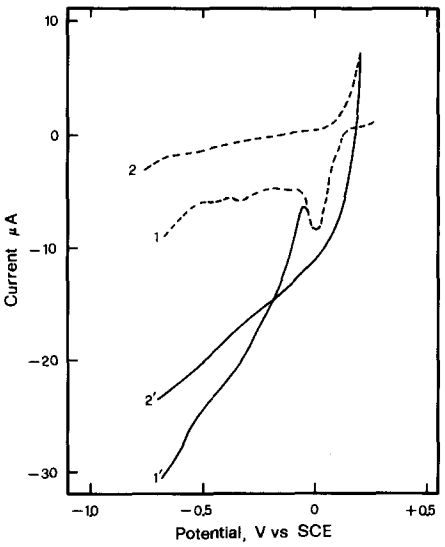

FIG. 2. Current–voltage curves of *p*-$FePSe_3$ in 0.5 *M* H_2SO_4–0.2 *M* $CuSO_4$. Curves 1 and 1′, curves during the first scan; curves 2 and 2′, curves during the second and later scans (1 and 2, dark; 1′ and 2′, light).

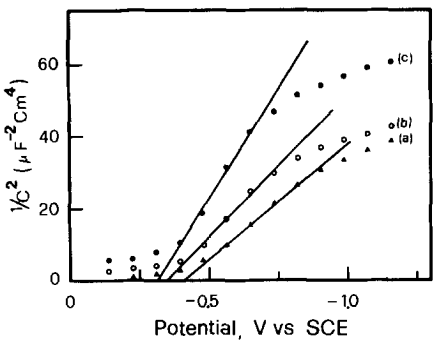

FIG. 3. Mott–Schottky plots of p-$FePSe_3$ in 0.5 M H_2SO_4 at frequencies (a) 2 kHz, (b) 10 kHz, and (c) 25 kHz.

band potential is -0.36 ± 0.05 V vs SCE. The majority carrier concentrations calculated from the slopes of the Mott–Schottky plots are in the range $0.8–1.5 \times 10^{17}$ cm^{-3}. This value is of the same order as that obtained from the measurement of the Hall coefficient at room temperature. ($R_H = 27$ cm^3/coulomb; $\mu \approx 1$ cm^2 V^{-1} sec^{-1}; $N = 2.5 \times 10^{17}$ cm^{-3}). The measured Hall mobility for $FePSe_3$ crystals did not vary significantly in the temperature range 300–160 K.

The spectral response (photocurrent vs λ) was measured at -0.85 and -0.9 V vs SCE for the selenide and the sulfide, respectively. The photocurrent quantum efficiencies, η (number of electrons flowing per incident photon), uncorrected for reflection at electrode surface, are plotted as a function of the incident photon energy in Fig. 4. The η values are very low for $FePS_3$. $FePSe_3$ shows higher quantum efficiencies consistent with its lower resistivity and narrower band gap. The Gärtner model has been applied to analyze the photocurrent across the semiconductor/electrolyte junction (*17, 18, 24–27*). In a simplified form the Gärtner equation may be written as

$$\eta = 1 - e^{-\alpha W}/(1 + \alpha L),$$

where η is the quantum efficiency, α is the optical absorption coefficient, W is the width of the depletion layer, and L is the diffusion length of the minority carrier. If both $\alpha W < 1$ and $\alpha L < 1$, η is proportional to α. The energy and the nature of the optical transitions are revealed by the dependence of the absorption coefficient α on the

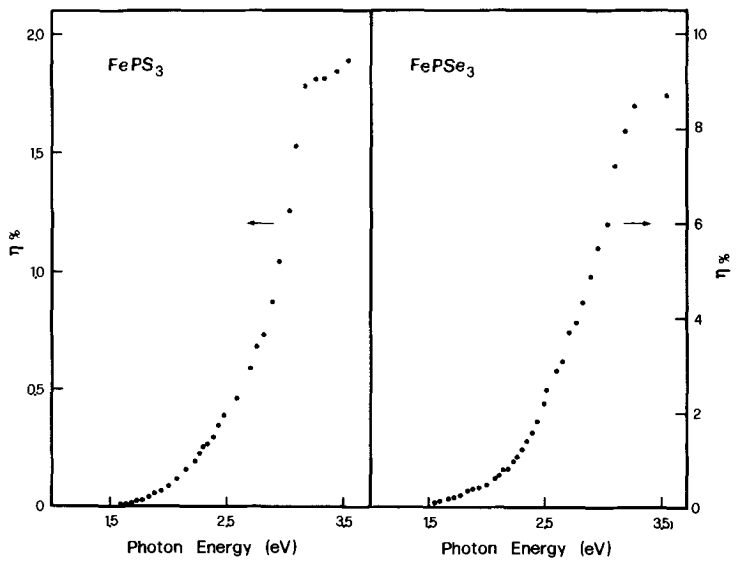

FIG. 4. Spectral response obtained as the variation of the quantum efficiency (η) with photon energy ($h\nu$) at an electrode potential of -0.9 V vs SCE for $FePS_3$ and -0.85 V vs SCE for $FePSe_3$.

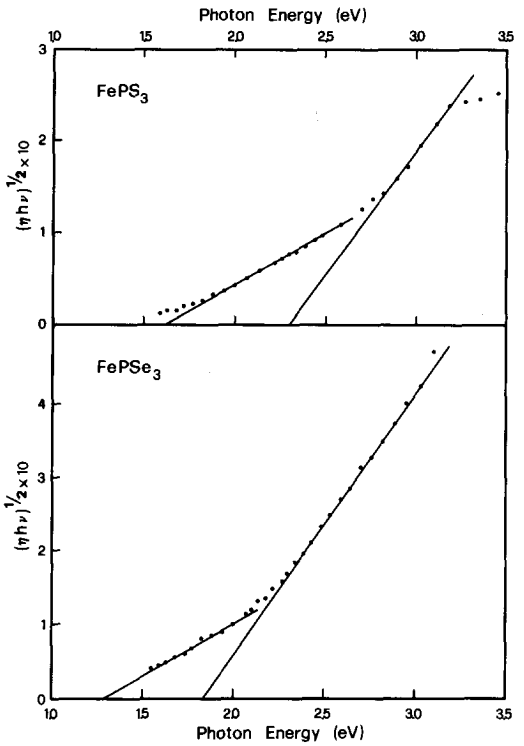

FIG. 5. The plot of $(\eta h\nu)^{1/2}$ vs photon energy ($h\nu$) for indirect optical transitions.

photon energy near the band edge, given by (*17*)

$$\alpha = A(h\nu - e_g)^{n/2}/h\nu,$$

where A is a constant factor. n is a constant such that $n = 1$ for direct allowed transitions, $n = 3$ for direct forbidden transitions, and $n = 4$ for indirect allowed transitions. Since η is proportional to α, the extrapolated intercept of the plot of $(\eta h\nu)^{2/n}$ vs $h\nu$ should give the energy of the band gap. Figure 5 shows the representation of $(\eta h\nu)^{0.5}(n = 4)$ vs $h\nu$ and this relationship with $n = 4$ appears to better fit the data. Two linear regions are identified and are interpreted as corresponding to two indirect band transitions. The lowest band gaps determined in this way, 1.3 eV for $FePSe_3$ and 1.62 eV for $FePS_3$, are in close agreement with those values reported in the literature and deduced from optical measurements (*3, 7*). The determination of the fundamental absorption edge is facilitated in the case of photocurrent spectra as measured here, since the *d–d* excitations do not contribute to the photocurrent. The crystal field splitted *d*-levels actually give discrete ground and excited states, characterized by very low carrier mobilities and therefore negligible contribution to the photocurrent by *d–d* transitions. But, in the optical spectra of the MPX_3 compounds, the *d–d* transitions occur close to the absorption edge and the intensity calculations become difficult (*3, 7*).

Discussion

The results can be explained on the basis of the energy band scheme proposed for MPX_3 layered compounds in relation to various spectroscopic studies (*9–11*). Assuming that the anion does not alter the main features, the band model for $FePX_3$ is drawn in Fig. 6. This is constructed from the energy levels of $[P_2X_6]^{4-}$ clusters with the localized *d*-levels of the divalent metal ions within the bonding–antibonding gap (*11*). The top of the valence band and the bottom of the conduction band consist of the bonding and antibonding orbitals of the P–P bond, respectively. The present measurement of a significant value (1 $cm^2\ V^{-1}\ sec^{-1}$) for the holes is indicative of a band conduction as can be expected in the narrow band of the P–P bonding states. This may be compared to the mobility value of ~2 $cm^2\ V^{-1}\ sec^{-1}$ for electrons measured by Foot and Nevett (*8*) for the *n*-doped $NiPS_3$ and interpreted to indicate band-like conduction. However, the density of states is much lower for the P–P bands (*11, 28*). The main valence band is, therefore, accepted to originate from the X $3p$ nonbonding states and it is not known to what extent the P–P bonding band overlaps the band of X $3p$ nonbonding states. Se in place of S

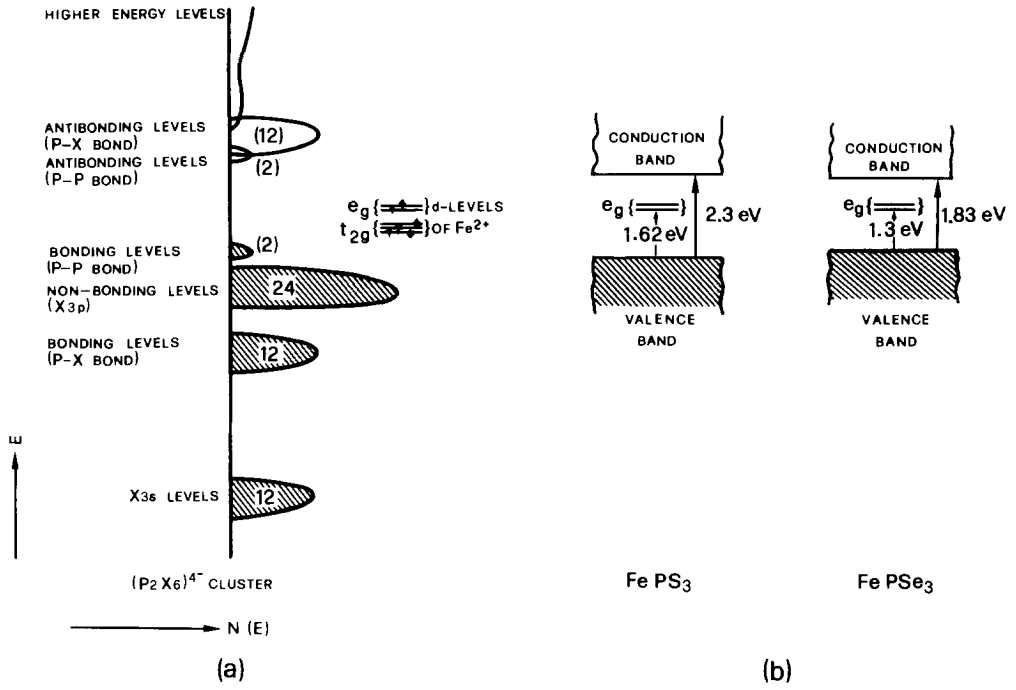

FIG. 6. (a) Energy level scheme of $FePX_3$ constructed from the energy levels of $[P_2X_6]^{4-}$ clusters and localized Fe^{2+} ions [from Ohno and Hirama (*11*)]. The figures in parentheses denote the electron occupancy per double formula and occupied states are shown. (b) Schematic diagram to indicate the transitions E_1 and E_2 (Table I).

TABLE I

ELECTRONIC PARAMETERS OF SOME MPX_3 LAYERED COMPOUNDS

MPX_3	E_1(eV)[a]	E_2(eV)[b]	Carrier mobility ($cm^2\ V^{-1}\ sec^{-1}$)	Reference
$ZnPS_3$	3.4	—	—	(*3*)
$CdPS_3$	3.5	—	—	(*3*)
$CdPSe_3$	2.27	—	—	(*23*)
$In_{2/3}PS_3$	3.1	—	—	(*3*)
$In_{2/3}PSe_3$	1.55	1.8	—	(*22*)
$MnPS_3$	3.0	—	—	(*3*)
$MnPSe_3$	1.87	—	—	(*23*)
$FePS_3$	1.5	—	—	(*3*)
	1.6	—	—	(*7*)
	1.62	2.3	0.5 (holes)[c]	This work
$FePSe_3$	1.3	—	—	(*3*)
	1.3	1.83	1.0 (holes)[c]	This work
$NiPS_3$	1.6	—	2.0 (electrons)[d]	(*7, 8*)

[a] E_1-band gap energy, taken to be the absorption edge measured from the optical spectra or the lowest energy transition determined from PEC measurements.

[b] E_2 higher energy transition determined from PEC measurements.

[c] Undoped (as grown) samples (p-type).

[d] Samples doped with Sc^{3+} (n-type) (Ref. (*8*)).

normally reduces the bonding–antibonding gap. Such a shift can increase the overlap between the P–P and Se $3p$ bands in comparison to the P–P and S $3p$ bands. The effect of selenium can be considered to raise the valence band of the selenide relatively to that of the sulfide.

In the absence of the localized d-levels, the energy gap evaluated for $NiPS_3$ is of the order of 2.6 eV (*11*). For $FePSe_3$ the gap should be smaller. The experimental values of the band gaps for various MPX_3 compounds are given in Table I. The discrete split d-levels lie within the bonding–antibonding gap and are progressively occupied by the d-electrons in the MPX_3 series (M = Mn, Fe, Ni). The transitions at lower energies 1.3 and 1.62 eV for $FePSe_3$ and $FePS_3$, respectively, can be interpreted

as transitions from the valence band to the d (t_{2g}, e_g) levels. The electrons excited to such levels are expected to be much less mobile. On the basis of tight binding band calculations on $FePS_3$, Whangbo *et al.* (*28*) have attributed the fundamental absorption edge at 1.62 eV to the transition from the valence band to the e_g levels of the octahedrally coordinated M^{2+} ion.

They have indicated that strong covalent interactions exist between iron and sulfur and that the t_{2g} levels form subbands mainly of metal 3d-orbital character while the e_g levels form subbands with strong sulfur lone pair character. The transition from the sulfur 3p valence band to the e_g bands are therefore favored. Nevertheless, the delocalization of the d-levels is limited so that the electrons remain prominently localized. The second indirect optical transitions at 1.83 eV ($FePSe_3$) and 2.3 eV ($FePS_3$) correspond to the transitions from the valence band to the conduction band. In the model established to account for the spectroscopic investigations (*11*), the low lying conduction bands for the MPX_3 series are considered to originate from the P–P and P–S antibonding levels, as outlined in Fig. 6. It is to be noted, however, that the results of Whangbo *et al.* (*28*) give a band picture in which the lowest conduction bands are formed by the 4s and 4p orbitals of the Fe^{2+} ions. More studies are needed to specify the disposition of the conduction bands. The localized nature of the d-electron states involved in the fundamental optical transition and the measured low mobilities of the charge carriers are the main reasons for the low values of quantum efficiencies measured here.

The electronic properties of the MPX_3 compounds are different from those of the MX_2 layered compounds (e.g., MoS_2, WSe_2) in which the d-levels overlap to form bands (*29*) and where optical transitions take place between bands. In the case of the MPX_3 compounds, the fundamental transition occurs between bands related to anion or phosphorus levels and localized d-levels. The nonbonding character of the states involved in the photoelectronic process can have a favorable influence on the stability of the crystal used as a cathode. With regard to the optical-to-chemical or electrical energy conversion in a PEC cell, the small values of the quantum efficiencies make these materials less attractive even though the band gaps are favorable. Also, the flat-band potentials are very near the hydrogen evolution potential. The current–voltage characteristics (Fig. 1) and the frequency dependence of the Mott–Schottky plots (Fig. 3) indicate the presence of surface states. The fact that the basal planar surfaces of the layered compounds are chemically inactive does not exclude that extrinsic surface states exist at the cleaved surfaces perpendicular to the c-axis. They are related to steps and dislocations on the surfaces as it has been considered for the MX_2 (e.g., WSe_2) compounds (*30, 31*). Also, for the MPX_3 compounds, the localized and incompletely filled d-states of the divalent metal ions that exist near the surface can play the role of surface states. From these considerations, it follows that any significant energy storage can be realized only after a suitable surface treatment is found in order to reduce the surface recombination.

Conclusion

The interpretation of the measured photoelectrochemical quantum efficiencies is proposed in terms of two indirect optical transitions at 1.3 and 1.83 eV for $FePSe_3$ and at 1.62 and 2.3 eV for $FePS_3$. The lowest energy transitions are in good agreement with the literature values based on optical studies. These are interpreted on the basis of the band scheme proposed for the MPX_3 layered compounds with localized d-levels. The quantum efficiencies are low

in most of the visible spectrum in agreement with the nature of the d-levels and with low carrier mobilities. The current–voltage and the flat-band potential measurements indicate significant surface recombination.

Acknowledgments

Thanks are due to Mr. Adam Feinar (ICP, EPFL) for help in the capacitance measurements with the Solartron spectrum analyzer in the IER, EPFL, and to Professor M. Grätzel and Dr. A. J. McEvoy (ICP) for the use of the setup for the spectral response measurements. A. Aruchamy acknowledges the EPFL for the support as Academic Guest in the Institut de Physique Appliquée.

References

1. A. H. Thompson and M. S. Whittingham, *Mater. Res. Bull.* **12,** 741 (1977).
2. A. Le Mehaute, G. Ouvrard, R. Brec, and J. Rouxel, *Mater. Res. Bull.* **12,** 1191 (1977).
3. R. Brec, D. M. Schleich, G. Ouvrard, A. Louisy, and R. Rouxel, *Inorg. Chem.* **18,** 1814 (1979).
4. M. S. Whittingham, *Prog. Solid State Chem.* **12,** 41 (1978).
5. R. Brec, G. Ouvrard, and J. Rouxel, *Mater. Res. Bull.* **20,** 1257 (1985).
6. F. Hülliger, *in* "Structural Chemistry of Layer-Type Phases" (F. Lévy, Ed.), p. 217, Reidel, Dordrecht (1976).
7. P. J. S. Foot, J. Suradi, and P. A. Lee, *Mater. Res. Bull.* **15,** 189 (1980).
8. P. J. S. Foot and B. A. Nevett, *Phys. Status Solidi A* **93,** 283 (1986).
9. F. S. Khumalo and H. P. Hughes, *Phys. Rev. B* **23,** 5375 (1981).
10. M. Piacentini, F. S. Khumalo, G. Leveque, C. G. Olson, and M. W. Lynch, *Chem. Phys.* **72,** 61 (1982); **72,** 289 (1982).
11. Y. Ohno and K. Hirama, *J. Solid State Chem.* **63,** 258 (1986).
12. A. J. Bard, A. B. Bocarsly, F.-R. F. Fan, E. G. Walton, and M. S. Wrighton, *J. Amer. Chem. Soc.* **102,** 3671 (1980).
13. J. A. Turner, J. Manassen, and A. J. Nozik, *Appl. Phys. Lett.* **37,** 488 (1980).
14. W. Kautek and H. Gerischer, *Ber. Bunsenges. Phys. Chem.* **84,** 645 (1980).
15. A. Heller, *Acc. Chem. Res.* **14,** 154 (1981).
16. M. Paranthaman, A. Aruchamy, G. Aravamudan, and G. V. Subba Rao, *Mater. Chem. Phys.* **14,** 349 (1986).
17. M. A. Butler, *J. Appl. Phys.* **48,** 1914 (1977).
18. F. P. Koffyberg, K. Dwight, and A. Wold, *Solid State Commun.* **30,** 433 (1979).
19. W. Kautek, H. Gerischer, and H. Tributsch, *J. Electrochem. Soc.* **127,** 2471 (1980).
20. B. L. Wheeler, G. Nagasubrananian, and A. J. Bard, *J. Electrochem. Soc.* **131,** 1038 (1984).
21. C. E. Byvik, B. Reichman, and D. W. Coleman, *J. Electrochem. Soc.* **129,** 237 (1982).
22. M. Etman, A. Katty, C. Levy-Clement, and P. Lemasson, *Mater. Res. Bull.* **17,** 579 (1982).
23. O. E. Hüsser, H. von Känel, and F. Lévy, *J. Electrochem. Soc.* **132,** 810 (1985).
24. W. W. Gärtner, *Phys. Rev.* **116,** 84 (1959).
25. J. Reichman, *Appl. Phys. Lett.* **36,** 574 (1980).
26. H. Reiss, *J. Electrochem. Soc.* **125,** 937 (1978).
27. R. H. Wilson, *J. Appl. Phys.* **48,** 4292 (1977).
28. M. H. Whangbo, R. Brec, G. Ouvrard, and J. Rouxel, *Inorg. Chem.* **24,** 2459 (1985).
29. C. F. Mattheis, *Phys. Rev. B* **8,** 3719 (1973).
30. H. J. Lewerence, H. Gerischer, and M. Lübke, *J. Electrochem. Soc.* **131,** 100 (1984).
31. A. J. Mc Evoy, M. Etman, and R. Memming, *J. Electroanal. Chem.* **190,** 225 (1985).